Journal Pre-proof

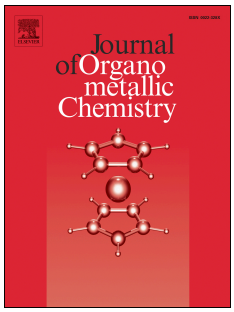

Synthesis, characterization and crystal structures of half-sandwich ruthenium complexes with bidentate chiral Schiff-base ligands

Chong Chen, Jiao Ji, Chang-Jiu Wang, Ai-Quan Jia, Qian-Feng Zhang

PII: S0022-328X(20)30030-9

DOI: https://doi.org/10.1016/j.jorganchem.2020.121129

Reference: JOM 121129

To appear in: *Journal of Organometallic Chemistry*

Received Date: 3 December 2019

Revised Date: 12 January 2020

Accepted Date: 18 January 2020

Please cite this article as: C. Chen, J. Ji, C.-J. Wang, A.-Q. Jia, Q.-F. Zhang, Synthesis, characterization and crystal structures of half-sandwich ruthenium complexes with bidentate chiral Schiff-base ligands, *Journal of Organometallic Chemistry* (2020), doi: https://doi.org/10.1016/j.jorganchem.2020.121129.

Synthesis, characterization and crystal structures of half-sandwich ruthenium complexes with bidentate chiral Schiff-base ligands

Chong Chen, Jiao Ji, Chang-Jiu Wang, Ai-Quan Jia, and Qian-Feng Zhang*

Institute of Molecular Engineering and Applied Chemistry, Anhui University of Technology, Ma'anshan, Anhui 243002, P R China

Condensation of salicylaldehyde or 5-nitrosalicylaldehyde with (*S*)-(+)-2-amino-3-methyl-1-butanol in refluxing ethanol afforded the chiral Schiff-base ligands (*S*)-*N*-(1-hydroxymethylisobutyl)salicylidene (**HL1***) and (*S*)-*N*-1-hydroxymethylisobutyl-5-nitrosalicylidene (**HL2***), respectively. Similarly, reaction of 3,5-di-*tert*-butylsalicylaldehyde or 3,5-dibromosalicylaldehyde with (*R*)-(+)-α-methylbenzylamine gave the chiral Schiff base ligands (*R*)-*N*-(1-phenylethyl)-3,5-di-*tert*-butylsalicylidene (**HL3***) and (*R*)-*N*-(1-phenylethyl)-3,5-dibromosalicylidene (**HL4***), respectively. Treatment of 3,5-dibromosalicylaldehyde with (*S*)-(+)-2-amino-1-propanol, (*S*)-(+)-2-amino-3-methyl-1-butanol or (*S*)-(-)-2-amino-3-phenyl-1-propanol in refluxing ethanol afforded (*S*)-*N*-(1-hydroxymethylethyl)-3,5-dibromosalicylidene (**HL5***), (*S*)-*N*-(1-hydroxymethylisobutyl)-3,5-dibromosalicylidene (**HL6***), and (*S*)-*N*-(1-hydroxymethylphenylethyl)-3,5-dibromosalicylidene (**HL7***), respectively. Interaction of $[(\eta^6\text{-}p\text{-cymene})RuCl_2]_2$ with two euivalents of the chiral Schiff-bases **HL1***–**HL7*** gave the corresponding half-sandwich ruthenium(II) complexes $[(\eta^6\text{-}p\text{-cymene})Ru(\kappa^2\text{-}N,O\text{-}\mathbf{L}^*)Cl]$ (**1**–**7**). The molecular structures of **HL1***–**HL7*** and the complex **3** have been determined by single-crystal X-ray crystallography.

Keywords: Half-sandwich ruthenium complex; Chiral Schiff base; Synthesis; Crystal structure

* Corresponding author. E-mail: zhangqf@ahut.edu.cn, ahutchang@yahoo.com (Q.-F. Zhang).

1. Introduction

The significance of catalysis in asymmetric synthesis has led to the development of numerous versatile chiral ligands [1−4]. Among them, chiral Schiff base ligands have attracted great attention for their applications in organic catalysis and stereochemical investigations [5,6]. It may be noted that bidentate chiral Schiff base ligands have various coordination mode, such as [*N*,*O*] [7], [*N*,*N*] [8] and [*N*,*P*] [9] and are readily modifiable to allow fine-tuning of steric and electronic properties for transition metal complexes, notably for ruthenium complexes [10,11]. A number of half-sandwich ruthenium complexes have been synthesized and applied to various organic transformations, such as C–N bond formation from imines and ketones [12], direct alkylation through C–H bond activation [13,14], olefin cyclopropanation [15] and transfer hydrogenation of ketones [16,17]. Brunner and coworkers reported [(η^6-*p*-cymene)Ru(LL*)(4-Mepy)](PF_6) (LL* = anion of (*S*)-(1-phenylethy1)salicylaldimine) [17] and [Ru(η^6-C_6H_6)(L–L)Cl] (L–L = (*S*)-*N*-(1-phenylethyl)salicylideneaminate) [18] and explored their stereochemistry and crystal structures. Previously, we have reported a series of new nitrosyl and triphenylphosphine ruthenium(II)/(III) complexes with three chiral *N*,*O*-chelate Schiff base ligands [19], as our long-standing research interest in ruthenium complexes with the potential catalytic properties, we disclose herein syntheses and structures of a series of half-sandwich ruthenium complexes with bidentate chiral Schiff base ligands derived from condensation of four different chiral amines (*R*)-(+)-α-methylbenzylamine, (*S*)-(+)-2-amino-3-methyl-1-butanol, (*S*)-(+)-2-amino-1-propanol, or (*S*)-(-)-2-amino-3-phenyl-1-propanol with salicylaldehyde or substituted salicylaldehyde in this paper.

2. Experimental

2.1. General considerations

All synthetic manipulations were carried out under dry nitrogen by standard Schlenk techniques. Solvents were purified by standard procedures and distilled prior to use. Triethylamine, salicylaldehyde, 5-nitrosalicylaldehyde, 3,5-di-*tert*-

butylsalicylaldehyde, 3,5-dibromosalicylaldehyde, (*R*)-(+)-α-methylbenzylamine, (*S*)-(+)-2-amino-3-methyl-1-butanol, (*S*)-(+)-2-amino-1-propanol and (*S*)-(-)-2-amino-3-phenyl-1-propanol were purchased from Alfa Aesar Ltd. and used without further purification. The starting ruthenium complex $[(\eta^6\text{-}p\text{-cymene})RuCl_2]_2$ was prepared according to the literature method [20]. NMR spectra were recorded on a Bruker ALX 400 Plus spectrometer operating at 400 MHz for ^{1}H and chemical shifts (δ, ppm) were reported with reference to $SiMe_4$ (^{1}H). Infrared spectra (KBr) were recorded on a Perkin-Elmer 16 PC FT-IR spectrophotometer with use of pressed KBr pellets. Electronic absorption spectra were obtained on a Shimadzu UV-2600 spectrophotometer. Elemental analyses were carried out using a Perkin-Elmer 2400 CHN analyzer.

*2.2. Synthesis of chiral Schiff base ligands (**HL1***–**HL7***)*

The chiral Schiff base ligands were synthesized by dissolving the corresponding salicyldehyde (2.0 mmol) in ethanol (20 mL), followd by slow addition of one equivalent of (*S*)-(+)-2-amino-3-methyl-1-butanol, (*R*)-(+)-α-methylbenzylamine, (*S*)-(+)-2-amino-1-propanol and (*S*)-(-)-2-amino-3-phenyl-1-propanol, respectively in ethanol (10 mL). The mixture was heated and refluxed for 4 h. After cooled to room temperature, the solvent was evaporated in *vacuo* and washed with cooled ethanol (5 mL × 3), and single crystals of **HL1***–**HL7*** were harvested from recrystallization of the seven chiral Schiff base ligands in methanol/dither ether (v/v = 1:3) at room temperature.

HL1*. Yield: 336 mg, 81%. ^{1}H NMR (400 MHz, DMSO-d_6, ppm): δ 12.85 (s, 1H, Ar−O*H*), 8.63 (s, 1H, C*H*=N), 7.62–6.92 (m, 4H, Ar–*H*), 4.26 (s, 1H, O*H*), 3.94 (d, *J* = 5.4 Hz, 2H, CH_2), 3.78 (m, 1H, C*H*), 1.92 (m, 1H, C*H*), 0.89 (d, *J* = 7.0 Hz, 6H, CH_3). IR (KBr disc, cm^{-1}): *v*(O–H) 3263 (s), *v*(C=N) 1619 (s), *v*(CH_3) 2962 (s), *v*(C–O) 1266 (s). Anal. calc. for $C_{12}H_{17}NO_2$: C, 69.48; H, 8.20; N, 6.75%. Found: C, 69.45; H, 8.22; N, 6.76%.

HL2*. Yield: 415 mg, 82%. ^{1}H NMR (400 MHz, DMSO-d_6, ppm): δ 13.31 (s, 1H, Ar−O*H*), 8.69 (s, 1H, C*H*=N), 8.47–7.51 (m, 3H, Ar–*H*), 4.24 (s, 1H, O*H*), 3.71 (d, *J* = 5.6 Hz, 2H, CH_2), 3.66 (m, 1H, C*H*), 2.12 (m, 1H, C*H*), 0.90 (d, *J* = 6.8 Hz, 6H, CH_3). IR (KBr disc, cm^{-1}): *v*(O–H) 3335 (s), *v*(CH_3) 2965 (s), *v*(C=N) 1629 (m), *v*(C=C) 1536 (s),

1488 (s), *v*(C–O) 1287 (s), *v*(Ar–NO_2) 1273 (s), 836 (s), 773 (s). Anal. calc. for $C_{12}H_{16}N_2O_4$: C, 57.08; H, 6.34; N, 11.10%. Found: C, 57.07; H, 6.34; N, 11.12%.

HL3*. Yield: 594 mg, 88%. ^{1}H NMR (400 MHz, C*D*Cl_3, ppm): δ 13.85 (s, 1H, Ar−O*H*), 8.65 (s, 1H, C*H*=N), 7.47–7.12 (m, 7H, Ar–*H*), 2.57 (m, 1H, C*H*), 1.63 (d, *J* = 4.2 Hz, 3H, CH_3), 1.50 (s, 9H, *t*-Bu), 1.34 (s, 9H, *t*-Bu). IR (KBr disc, cm^{-1}): *v*(CH_3) 2963 (s), *v*(CH_2) 2906 (s), 2842 (s), *v*(C=N) 1629 (s), *v*(C=C) 1583 (s), 1467 (s), 1451 (s), *v*(C–O) 1250 (s). Anal. calc. for $C_{23}H_{31}NO$: C, 81.78; H, 9.19; N, 4.15%. Found: C, 81.77; H, 9.18; N, 4.16%.

HL4*. Yield: 598 mg, 78%. ^{1}H NMR (400 MHz, DMSO-d_6, ppm): δ 13.57 (s, 1H, Ar−O*H*), 8.54 (s, 1H, C*H*=N), 7.65–7.32 (m, 7H, Ar–*H*), 2.42 (m, 1H, C*H*), 1.56 (d, *J* = 4.2 Hz, 3H, CH_3). IR (KBr disc, cm^{-1}): *v*(O–H) 3261 (br), *v*(CH_2) 2906 (s), 2842 (s), *v*(C=N) 1620 (s), *v*(C=C) 1571 (s), 1475 (s), *v*(C–O) 1266 (s) *v*(Ar–Br) 615 (s), 558 (s). Anal. calc. for $C_{15}H_{13}NOBr_2$: C, 47.0; H, 3.39; N, 3.66%. Found: C, 47.06; H, 3.38; N, 3.67%.

HL5*. Yield: 555 mg, 82%. ^{1}H NMR (400 MHz, DMSO-d_6, ppm): δ 14.98 (s, 1H, Ar−O*H*), 8.53 (s, 1H, C*H*=N), 7.84–7.70 (m, 2H, Ar–*H*), 4.24 (s, 1H, O*H*), 3.96 (d, *J* = 3.6 Hz, 2H, CH_2), 3.24 (m, 1H, C*H*), 1.35 (d, *J* = 2.6 Hz, 3H, CH_3). IR (KBr disc, cm^{-1}): *v*(O–H) 3261 (br), *v*(CH_3) 2963 (s), *v*(CH_2) 2906 (s), 2842 (s), *v*(C=N) 1618 (s), *v*(C=C) 1586 (s), 1470 (s), *v*(C–O) 1259 (s), *v*(Ar–Br) 596 (s), 568 (s). Anal. calc. for $C_{10}H_{11}NO_2Br_2 \cdot 0.25H_2O$: C, 35.17; H, 3.39; N, 4.10%. Found: C, 35.13; H, 3.36; N, 4.11%.

HL6*. Yield: 614 mg, 84%. ^{1}H NMR (400 MHz, DMSO-d_6, ppm): δ 15.08 (s, 1H, Ar−O*H*), 8.61 (s, 1H, C*H*=N), 7.84–7.70 (m, 2H, Ar–*H*), 4.24 (s, 1H, O*H*), 3.96 (d, *J* = 4.5 Hz, 2H, CH_2), 3.71 (m, 1H, C*H*), 1.94 (m, 1H, C*H*), 0.88 (d, *J* = 4.8 Hz, 6H, CH_3). IR (KBr disc, cm^{-1}): *v*(O–H) 3261 (s), *v*(CH_3) 2963 (s), *v*(C=N) 1634 (s), *v*(C=C) 1571 (s), 1475 (s), *v*(C–O) 1249 (s), *v*(Ar–Br) 612 (s), 577 (s). Anal. calc. for $C_{12}H_{15}NO_2Br_2$: C, 39.45; H, 4.11; N, 3.84%. Found: C, 39.47; H, 4.10; N, 3.85%.

HL7*. Yield: 702 mg, 85%. ^{1}H NMR (400 MHz, DMSO-d_6, ppm): δ 14.84 (s, 1H, Ar−O*H*), 8.46 (s, 1H, C*H*=N), 7.82–7.23 (m, 7H, Ar–*H*), 4.26 (s, 1H, O*H*), 3.96 (d, *J* = 3.4 Hz, 2H, CH_2O), 3.71 (m, 1H, C*H*), 3.52 (d, *J* = 5.2 Hz, 2H, CH_2Ph). IR (KBr disc,

cm^{-1}): *v*(O–H) 3261 (s), *v*(CH_2) 2906 (s), 2842 (s), *v*(C=N) 1616 (s), *v*(C=C) 1571 (s), 1475 (s), *v*(C–O) 1271 (s), *v*(Ar–Br) 603 (s), 567 (s). Anal. calc. for $C_{16}H_{15}NO_2Br_2$: C, 46.49; H, 3.63; N, 3.39%. Found: C, 46.48; H, 3.63; N, 3.41%.

*2.3. Synthesis of (S)-[(η^6-p-cymene)Ru(κ^2-N,O-**L1***)Cl] (**1**)*

To a solution of [(η^6-*p*-cymene)$RuCl_2$]$_2$ (62 mg, 0.10 mmol) in tetrahydrofuran (20 mL) was added a solution of **HL1*** (42 mg, 0.20 mmol) and Et_3N (22 mg, 0.20 mmol) in tetrahydrofuran (5 mL), and then the mixture was heated at 90 °C with stirring overnight, during which time there was a color change from yellow to orange. After removal of solvent in *vacuo*, the resulting orange powder of **1** was washed with diethyl ether (5 mL × 3) and dried in *vacuo*. Yield: 39 mg, 82% (based on Ru). ^{1}H NMR (400 MHz, C*D*Cl_3, ppm): δ 8.25 (s, 1H, C*H*=N), 7.06–7.28 (m, 4H, Ar–*H*), 5.24–5.52 (m, 4H, *p*-cymene), 4.26 (s, 1H, O*H*), 2.85 (d, *J* = 6.8 Hz, 2H, CH_2), 2.29 (m, 1H, C*H*), 2.16 (m, 1H, C*H*), 2.03 (m, 1H, C*H*), 1.21 (m, 6H, CH_3), 1.19 (d, *J* = 6.8 Hz, 6H, CH_3), 1.12 (s, 1H, CH_3). IR (KBr disc, cm^{-1}): *v*(O–H) 3189 (s), *v*(C=N) 1650 (s), *v*(Ar–O) 1240 (s). Anal. calc. for $C_{22}H_{29}NO_2ClRu$: C, 55.49; H, 6.10; N, 2.94; O, 6.73%. Found: C, 55.48; H, 6.08; N, 2.95; O, 6.74%.

*2.4. Synthesis of (S)-[(η^6-p-cymene)Ru(κ^2-N,O-**L2***)Cl] (**2**)*

A mixture of [(η^6-*p*-cymene)$RuCl_2$]$_2$ (62 mg, 0.10 mmol), **HL2*** (51 mg, 0.20 mmol) and Et_3N (22 mg, 0.20 mmol) in tetrahydrofuran (25 mL) was heated at reflux with stirring overnight, during which time the color changed from orange to red-brown. The solvent was removed in *vacuo*, and the residue was washed with diethyl ether (5 mL × 3) and dissolved in dichloromethane (2 mL). *n*-Hexane (10 mL) was added to the solution to precipitate the complex which was isolated and washed with diethyl ether (5 mL × 3) and finally dried in *vacuo*. Yield: 41 mg, 80% (based on Ru). ^{1}H NMR (400 MHz, C*D*Cl_3, ppm): δ 8.32 (s, 1H, C*H*=N), 7.31–7.16 (m, 3H, Ar–*H*), 5.39–5.33 (m, 4H, *p*-cymene), 4.02 (s, 1H, O*H*), 2.90 (d, *J* = 21.8 Hz, 2H, CH_2), 2.26 (s, 1H, C*H*), 2.06 (m, 1H, C*H*), 2.03 (s, 1H, C*H*), 1.32 (m, 6H, CH_3), 1.28 (s, 3H, CH_3), 0.94 (d, *J* = 6.8 Hz, 6H,

CH_3). IR (KBr disc, cm^{-1}): ν(O–H) 3189 (s), ν(C=N) 1650 (s), ν(Ar–NO_2) 1526 (s), ν(Ar–O) 1261 (s). Anal. calc. for $C_{22}H_{28}N_2O_4ClRu$: C, 50.69; H, 5.38; N, 5.38; O, 12.29%. Found: C, 50.67; H, 5.38; N, 5.37; O, 12.28%.

*2.5. Synthesis of (R)-[(η^6-p-cymene)Ru(κ^2-N,O-**L3***)Cl] (**3**)*

To a solution of [(η^6-*p*-cymene)$RuCl_2$]$_2$ (62 mg, 0.10 mmol) in tetrahydrofuran (20 mL) was added a solution of **HL3*** (68 mg, 0.20 mmol) and Et_3N (22 mg, 0.20 mmol) in tetrahydrofuran (5 mL), and then the mixture was heated at 90 °C with stirring overnight, during which there was a color change from yellow to orange. After removal of solvent in *vacuo*, the residue was dissolved in dichloromethane (3 mL) and the solution was filtered. The filtrate was layered with *n*-hexane (20 mL) at room temperature, and light red block-shaped crystals of (*S*)-[(η^6-*p*-cymene)Ru(κ^2-*N*,*O*-**L3***)Cl] (**3**) were obtained in five days. Yield: 27 mg, 43% (based on Ru). ^{1}H NMR (400 MHz, C*D*Cl_3, ppm): δ 8.16 (s, 1H, C*H*=N), 7.23–7.16 (m, 2H, Ar–*H*), 6.52–5.94 (m, 5H, Ar–*H*), 5.22–5.00 (m, 4H, *p*-cymene), 2.96 (s, 1H, C*H*), 2.21 (d, *J* = 29.4 Hz, 3H, CH_3), 2.12–1.89 (m, 6H, CH_3), 1.86 (s, 3H, CH_3), 1.25 (d, *J* = 20.8 Hz, 18H, *t*-Bu). IR (KBr disc, cm^{-1}): ν(O–H) 3253 (s), ν(C=N) 1629 (s), ν(*t*-Bu) 1381 (s), 1362 (vs), ν(Ar–O) 1276 (s). Anal. calc. for $C_{33}H_{44}NOClRu$: C, 65.22; H, 7.25; N, 2.31; O, 2.64%. Found: C, 65.20; H, 7.25; N, 2.33; O, 2.65%.

*2.6. Synthesis of (R)-[(η^6-p-cymene)Ru(κ^2-N,O-**L4***)Cl] (**4**)*

A mixture of [(η^6-*p*-cymene)$RuCl_2$]$_2$ (62 mg, 0.10 mmol), **HL4*** (77 mg, 0.20 mmol) and Et_3N (22 mg, 0.20 mmol) in tetrahydrofuran (25 mL) was heated at reflux with stirring overnight, during which time the color changed from orange to dark red. After removal of solvent in *vacuo*, dichloromethane (10 mL) was added and the solution was filtered. The filtrate was concentrated and the residue was washed with diethyl ether (5 mL × 2) and *n*-hexane (5 mL × 2). Recrystallization from dichloromethane/*n*-hexane (1:5) afforded dark red solids of **4**. Yield: 51 mg, 79% (based on Ru). ^{1}H NMR (400 MHz, C*D*Cl_3, ppm): δ 8.36 (s, 1H, C*H*=N), 7.26 (m, 5H, Ar–*H*), 7.15 (m, 2H, Ar–*H*), 5.47–5.19

(m, 4H, *p*-cymene), 2.36 (m, 1H, C*H*), 1.36 (m, 6H, CH_3), 1.25 (d, *J* = 3.4 Hz, 3H, CH_3), 1.23 (s, 1H, C*H*), 0.92 (d, *J* = 6.8 Hz, 3H, CH_3). IR (KBr disc, cm^{-1}): *v*(C=N) 1659 (s), *v*(Ar–O) 1315 (s). Anal. calc. for $C_{25}H_{25}NOClBr_2Ru$: C, 46.04; H, 3.84; N, 2.15; O, 2.46%. Found: C, 46.05; H, 3.84; N, 2.17; O, 2.45%.

*2.7. Synthesis of (S)-[(η^6-p-cymene)Ru(κ^2-N,O-**L5***)Cl] (**5**)*

To a solution of [(η^6-*p*-cymene)$RuCl_2$]$_2$ (62 mg, 0.10 mmol) in tetrahydrofuran (20 mL) was added a solution of **HL5*** (67 mg, 0.20 mmol) and Et_3N (22 mg, 0.20 mmol) in tetrahydrofuran (5 mL), and then the mixture was heated at 90 °C with stirring overnight, during which there was a color change from orange to dark red. After removal of solvent in *vacuo*, the residue was washed with diethyl ether (5 mL × 3). Recrystallization from dichloromethane/*n*-hexane (1:5) gave dark red solids of **5**. Yield: 46 mg, 76% (based on Ru). ^{1}H NMR (400 MHz, C*D*Cl_3, ppm): δ 8.29 (s, 1H, C*H*=N), 7.22–7.01 (m, 2H, Ar–*H*), 5.54–5.33 (m, 4H, *p*-cymene), 4.10 (s, 1H, O*H*), 3.88 (d, *J* = 6.6 Hz, 2H, CH_2), 2.32 (m, 1H, C*H*), 1.35 (d, *J* = 6.9 Hz, 6H, CH_3), 1.25 (d, *J* = 4.6 Hz, 3H, CH_3), 1.23 (s, 1H, C*H*), 1.23–1.18 (m, 3H, CH_3). IR (KBr disc, cm^{-1}): *v*(O–H) 3256 (s), *v*(C=N) 1613 (s), *v*(Ar–O) 1314 (s). Anal. calc. for $C_{20}H_{23}NO_2ClBr_2Ru$: C, 39.64; H, 3.80; N, 2.31; O, 5.28%. Found: C, 39.63; H, 3.79; N, 2.33; O, 5.27%.

*2.8. Synthesis of (S)-[(η^6-p-cymene)Ru(κ^2-N,O-**L6***)Cl] (**6**)*

To a solution of [(η^6-*p*-cymene)$RuCl_2$]$_2$ (62 mg, 0.10 mmol) in tetrahydrofuran (20 mL) was added a solution of **HL6*** (73 mg, 0.20 mmol) and Et_3N (22 mg, 0.20 mmol) in tetrahydrofuran (5 mL), and then the mixture was heated at 90 °C with stirring overnight, during which there was a color change from orange to dark red-brown. After removal of solvent in *vacuo*, the residue was washed with diethyl ether (5 mL × 3) and *n*-hexane (3 mL × 3). The desired product **5** was obtained by recrystallization from dichloromethane/*n*-hexane (1:5). Yield: 51 mg, 81% (based on Ru). ^{1}H NMR (400 MHz, C*D*Cl_3, ppm): δ 8.24 (s, 1H, C*H*=N), 7.26–7.09 (m, 2H, Ar–*H*), 5.69–5.43 (m, 4H, *p*-cymene), 4.22 (s, 1H, O*H*), 3.23 (d, *J* = 3.5 Hz, 2H, CH_2), 2.46 (m, 1H, C*H*), 2.31 (s, 1H,

C*H*), 2.17–2.09 (m, 6H, CH_3), 1.19 (s, 3H, CH_3), 1.18 (m, 1H, C*H*), 1.13 (d, J = 10.0 Hz, 6H, CH_3). IR (KBr disc, cm^{-1}): ν(O–H) 3223 (s), ν(C=N) 1606 (s), ν(Ar–O) 1256 (s). Anal. calc. for $C_{22}H_{27}NO_2ClBr_2Ru$: C, 41.67; H, 4.26; N, 2.21; O, 5.05%. Found: C, 41.66; H, 4.26; N, 2.22; O, 5.06%.

*2.9. Synthesis of (S)-[(η^6-p-cymene)Ru(κ^2-N,O-**L7***)Cl] (**7**)*

A mixture of [(η^6-*p*-cymene)$RuCl_2$]$_2$ (62 mg, 0.10 mmol), **HL7*** (83 mg, 0.20 mmol) and Et_3N (22 mg, 0.20 mmol) in tetrahydrofuran (25 mL) was heated at reflux with stirring overnight, during which time the color changed from orange to dark red. After removal of solvent in *vacuo*, dichloromethane (5 mL) was added and the solution was filtered. The filtrate was concentrated and the residue was washed with diethyl ether (5 mL × 2) and *n*-hexane (5 mL × 2). Recrystallization from dichloromethane/*n*-hexane (1:5) afforded dark red solids of **7**. Yield: 51 mg, 75% (based on Ru). ^{1}H NMR (400 MHz, C*D*Cl_3, ppm): δ 8.33 (s, 1H, C*H*=N), 7.33–7.19 (m, 5H, Ar–*H*), 7.18 (m, 2H, Ar–*H*), 5.56–5.24 (m, 4H, *p*-cymene), 4.12 (s, 1H, O*H*), 3.20 (d, J = 3.2 Hz, 2H, CH_2), 2.93 (s, 1H, C*H*), 2.38 (m, 1H, C*H*), 1.32–1.28 (m, 6H, CH_3), 0.93 (m, 3H, CH_3). IR (KBr disc, cm^{-1}): ν(O–H) 3230 (s), ν(C=N) 1649 (s), ν(Ar–O) 1236 (s). Anal. calc. for $C_{26}H_{27}NO_2ClBr_2Ru$: C, 45.78; H, 3.96; N, 2.05; O, 4.70%. Found: C, 45.77; H, 3.96; N, 2.05; O, 4.71%.

2.10. X-Ray crystallography

A summary of crystallographic data and experimental details for ligands **HL1***–**HL7*** and complex **3** are summarized in Table 1. The structure of **HL2*** was included for completion only. Intensity data were collected on a Bruker SMART APEX 2000 CCD diffractometer using graphite-monochromated Mo-K radiation (λ = 0.71073 Å) at 296(2) K. The collected frames were processed with the software SAINT [21]. The data was corrected for absorption using the program SADABS [22]. Structures were solved by the direct methods and refined by full-matrix least-squares on F^2 using the SHELXTL software package [23,24]. All non-hydrogen atoms were refined anisotropically. The

positions of all hydrogen atoms were generated geometrically (C_{sp3}–H = 0.96 and C_{sp2}–H = 0.93 Å) and included in the structure factor calculations with assigned isotropic thermal parameters but were not refined.

3. Results and discussion

As shown in Scheme 1, the chiral Schiff-base ligands **HL1***–**HL7*** were synthesized from the condensation of the corresponding salicylaldehyde and its derivatives with four different chiral amines (*S*)-2-amino-3-methylbutan-1-ol, (*R*)-(+)-α-methylbenzylamine, (*S*)-(+)-2-amino-1-propanol and (*S*)-(-)-2-amino-3-phenyl-1-propanol, respectively, in moderate to high yields. Treatment of $[(\eta^6\text{-}p\text{-cymene})RuCl_2]_2$ with two equivalent chiral Schiff base ligands **HL1***–**HL7*** in the presence of triethylamine in tetrahydrofuran under reflux afforded the half-sandwich ruthenium complexes (*S*)-$[(\eta^6\text{-}p\text{-cymene})Ru(\kappa^2\text{-N,O-}\mathbf{L1}^*)Cl]$ (**1**), (*S*)-$[(\eta^6\text{-}p\text{-cymene})Ru(\kappa^2\text{-N,O-}\mathbf{L2}^*)Cl]$ (**2**), (*R*)-$[(\eta^6\text{-}p\text{-cymene})Ru(\kappa^2\text{-N,O-}\mathbf{L3}^*)Cl]$ (**3**), (*R*)-$[(\eta^6\text{-}p\text{-cymene})Ru(\kappa^2\text{-N,O-}\mathbf{L4}^*)Cl]$ (**4**), (*S*)-$[(\eta^6\text{-}p\text{-cymene})Ru(\kappa^2\text{-N,O-}\mathbf{L5}^*)Cl]$ (**5**), (*S*)-$[(\eta^6\text{-}p\text{-cymene})Ru(\kappa^2\text{-N,O-}\mathbf{L6}^*)Cl]$ (**6**) and (*S*)-$[(\eta^6\text{-}p\text{-cymene})Ru(\kappa^2\text{-N,O-}\mathbf{L7}^*)Cl]$ (**7**) (Scheme 2), respectively. The two bridged chloro ligands in $[(\eta^6\text{-}p\text{-cymene})RuCl_2]_2$ were replaced by one monoanionic $\mathbf{L}^{*-}$ ligand without chiral inversion. The chiral Schiff base ligands **L1***–**L7*** in complexes **1**–**7** all serve as *N*,*O*-bidentate ligands, similar to those in the other reported ruthenium complexs with chiral Schiff base ligands $[(\eta^6\text{-}p\text{-cymene})Ru\{2\text{-}O\text{-}(3,5\text{-di-}t\text{-Bu})C_6H_2CH{=}NCH(Me)Ph\}Cl]$ [25], [Ru(Sal val)(PPh_3)(bipy)] (Sal = salicylaldehyde, val = L-valine) [26] and $[(\eta^6\text{-}p\text{-cymene})Ru(\mathbf{3}\text{-}H^+)Cl]$ (**3** = (*S*)-2-methoxy-2'-(2-hydroxybenzylidenamino)-1,1'-binaphthyl) [27]. The half-sandwich ruthenium complexes **1**–**7** are air and moisture stable, soluble in dichloromethane, chloroform, acetone and alcohol.

IR spectra of chiral Schiff base ligands **HL1***–**HL7*** and half-sandwich ruthenium complexes **1**–**7** all showed the CH=N groups at around 1620 cm^{-1}, which is characteristic of the azomethine group absorptions [28]. The strong absorption at the region 1249–1287 cm^{-1} in **HL1***–**HL7*** belong to the stretching vibration of C(Ar)–OH. Similar absorption peaks of C(Ar)–O are observed in the spectra of complexes **1**–**7**. The chiral ligands

HL4*–**HL7*** with dibromo substitutes show two medium peaks at 615 and 578 nm for **HL4***, 596 and 568 nm for **HL5***, 603 and 567 nm for **HL6*** and 612 and 577 nm for **HL7***, which are attributed to the stretching vibration of C(Ar)–Br [29]. The aldimine (–C*H*=N–) proton resonances of **HL1***–**HL7*** are at the region of 8.46–8.53 ppm. The chemical shift of Ar–*H* was found at 7.62–6.92 ppm for **HL1*** and 8.47–7.51 ppm for **HL2***, possibly due to the electron-withdrawing property of $–NO_2$ group. Figs. 1 and 2 show the UV/Vis spectra of the chiral Schiff base ligands **HL1***–**HL7*** and the half-sandwich ruthenium(II) complexes **1**–**7** in dichloromethane, respectively. The bands at around 285 nm of complexes **1**–**7** are assigned to $\pi\rightarrow\pi^*$ transition of the azomethine chromophore and there is a blue shift of about 40 nm compared with the free chiral Schiff base ligands (325 nm), possibly due to the coordination influence [30]. The peaks in the region of 365–400 nm could be attributed to MLCT (metal-to-ligand charge transfer) transition in complexes **1**–**7**, in which complex **3** (365 nm) has a 20 nm blue shift compared to complex **1** (385 nm), possibly due to the electron donating ability of the *tert*-butyl groups. Conversely, complex **2** and **4**–**7** (about 395 nm) have a 10 nm red shift compared to that of **1**, due to the electron withdrawing ability of the nitro group and bromo groups, respectively. This phenomenon could be ascribed to the lower electronegativity and higher LUMO energy of **L3***$^-$ and the opposite trend for **L2***$^-$ and **L4***$^-$–**L7***$^-$ [31].

The structures of chiral Schiff base ligands **HL1***–**HL7*** and complex **3** have been established by X-ray crystallography. The perspective views of the molecular structures of ligands **HL1***–**HL7*** and complex **3** are shown in Figs. 3–10, respectively, with atom numbering scheme. The packing modes of the ligands (see Figs. S1–S7) clearly show the intramolecular hydrogen bonds with the intramolecular O–H···N distances in **HL1***–**HL7*** being 1.69, 1.86, 1.72, 1.88, 1.82, 1.85 and 1.82 Å, respectively. Expect for **HL3***, the chiral ligands also have intermolecular hydrogen bonds and the distances of O–H···O are in the range of 1.74–1.97 Å. The crystals of complex **3** belong to triclinic space group $P\bar{1}$ and both the ruthenium center and the C* of **L3*** adopt *R*-configuration ((R_{Ru}, R_C)-**3**). Selected bond lengths and bond angles for **3** are summarized in the caption of Fig. 10. The configuration of ruthenium atom is obtained using a priority sequence: η^6-*p*-cymene > Cl > O (L–L) > N (L–L) [32] and the asymmetric carbon atom in the chiral

Schiff base ligand has the expected R_C-configuration without chiral inversion. The bond lengths of C=N is 1.303(7) Å, which is a little longer than that in the uncoordinated chiral Schiff base ligand (1.265(4) Å). The molecular structure in the crystal clearly shows that (R_{Ru}, R_C)-**3** consists of a *p*-cymene ligand, a terminal chlolo ligand and a bidentate *N*,*O*-donor chelating ligand **L3***$^-$. The ruthenium center is in a slightly distorted octahedral coordination environment and has six-coordinate geometry assuming that the *p*-cymene ring serve as a three-coordinated ligand, which is common for half-sandwich "piano-stool" structures [33–37]. The average of the Ru–C bond lengths (*p*-cymene ring) is 2.198(6) Å, which is about 0.036 Å longer than that in the η^6-C_6H_6 complex (2.162(9) Å), indicative of the higher Lewis basicity of the dialkyl substitution of the η^6-*p*-cymene ligand with respect to the η^6-*p*-benzene ligand [18]. The Ru–O and Ru–N bond lengths are 2.054(4) and 2.117(5) Å, respectively, similar to other half-sandwich ruthenium complexes with *N*,*O*-chelated Schiff base ligands, such as (2.057(3) and 2.096(3) Å) [38]. The ligand **L3***$^-$ coordinated with central ruthenium atom and formed a six-membered planar ring (mean deviation, 0.0354 Å), which makes a dihedral angle of 5.428(11)° with the phenyl ring of the salicylaldehyde ligand. The bite N–Ru–O angle is 88.21(17)°, which is a little bigger than those in half-sandwich ruthenium complexes with (*S*)-*N*-(1-phenylethyl)salicylideneamine ligands (83.2°–86.8°) [18, 39]. The 1-phenylethyl group at the chiral carbon atom is almost perpendicular to the chelate plane (dihedral angles 78.44(23)^o) and in a position for the stabilizing interaction with the π-bonded *p*-cymene ligand, called "*β*-phenyl effect" [39]. The distances from the centroid of the cymene ring (C^0_{Ph}) to the H and Me at the chiral carbon are 3.472 and 4.928 Å respectively, indicative of a geometry that close to the cymene ring for C*–H [25].

In summary, a series of bidentate chiral Schiff base ligands and corresponding half-sandwich ruthenium(II) complexes were synthesized. The molecular structures of **HL1***–**HL7*** and complex **3** have been determined by single-crystal X-ray crystallography. The chiral Schiff base ligands have intramolecular O–H···N hydrogen bonds in the range of 1.69–1.88 Å, and intermolecular O–H···O in the range of 1.74–1.97 Å. UV/Vis spectra of complexes **1**–**7** show a blue shift of about 40 nm compared with the corresponding free chiral Schiff base ligands. The peak at 365 nm of complex **3** is

assigned to a MLCT transition, which has a blue shift compared with the other presented ruthenium complexes, possibly due to the lower electronegativity and higher LUMO energy of **L3***$^{-}$ with *tert*-butyl groups [31]. In complex **3**, the ruthenium atom adopts *R*-configuration and the R_c-configuration possibly suggested that formation of the ruthenium complexes proceeded without chiral inversion [19]. The 1-phenylethyl group attached to the chiral carbon is in a position for the stabilizing interaction with the η^6-*p*-cymene ligand in complex **3**, which is generally observed for half-sandwich ruthenium complexes subject to "*β*-phenyl effect" [39]. Exploration of ruthenium complexes as catalysts for asymmetric synthesis is underway in our laboratory.

Supplementary material

Crystallographic data for (*S*)-*N*-(1-hydroxymethylisobutyl)salicylidene (**HL1***), (*S*)-*N*-(1-hydroxymethylisobutyl)-5-nitrosalicylidene (**HL2***), (*R*)-*N*-(1-phenylethyl)-3,5-di-*tert*-butylsalicylidene (**HL3***), (*R*)-*N*-(1-phenylethyl)-3,5-dibromosalicylidene) (**HL4***), (*S*)-*N*-(1-hydroxymethylethyl)-3,5-dibromosalicylidene (**HL5***), (*S*)-*N*-(1-hydroxymethylisobutyl)-3,5-dibromosalicylidene (**HL6***), (*S*)-*N*-(1-hydroxymethylphenylethyl)-3,5-dibromosalicylidene (**HL7***) and (*R*)-[(η^6-*p*-cymene)Ru(κ^2-*N*,*O*-**L3***)Cl] (**3**) have been deposited with the Cambridge Crystallographic Data Centre as supplementary publication nos. CCDC 1969259-1969266, respectively. Copies of the data can be obtained free of charge on application to CCDC, 12 Union Road, Cambridge CB2 1EZ, UK [fax: (+44)1233-336-033; e-mail: deposit@ccdc.cam.ac.uk].

Acknowledgements

This project was supported by the Natural Science Foundations of China (21372007).

References

[1] H.-N. Chai, T.-T. Liu, Z.-K. Yu, NHTs effect on the enantioselectivity of Ru(II) complex catalysts bearing a chiral bis(NHTs)-substituted imidazolyl-oxazolinyl-pyridine ligand for asymmetric transfer hydrogenation of ketones, Organometallics 36 (2017) 4136−4144.

[2] Z.-Y. Zheng, Y.-X. Cao, Q.-L. Chong, Z.-B. Han, J.-M. Ding, C.-G. Luo, Z. Wang, D.-S. Zhu, Q.-L. Zhou, K.-L. Ding, Chiral cyclohexyl-fused spirobiindanes: practical synthesis, ligand development, and asymmetric catalysis, J. Am. Chem. Soc. 140 (2018) 10374−10381.

[3] K. Imai, Y. Takayama, H. Murayama, H. Ohmiya, Y. Shimizu, M. Sawamura, Asymmetric synthesis of α-alkylidene-β-lactams through copper catalysis with a prolinol-phosphine chiral ligand, Org. Lett. 21 (2019) 1717−1721.

[4] H.C. Kolb, M.S. VanNieuwenhze, K.B. Sharpless, Catalytic asymmetric dihydroxylation, Chem. Rev. 94 (1994) 2483−2547.

[4] T. Tanaka, Y. Yasuda, M. Hayashi, New chiral Schiff base as a tridentate ligand for catalytic enantioselective addition of diethylzinc to aldehydes, J. Org. Chem. 71 (2006) 7091−7093.

[5] G.-Y. Li, J. Zhang, P.W.H. Chan, Z.-J. Xu, N.-Y. Zhu, C.-M. Che, Enantioselective intramolecular cyclopropanation of *cis*-alkenes by chiral ruthenium(II) Schiff base catalysts and crystal structures of (Schiff base)ruthenium complexes containing carbene, PPh_3, and CO ligands, Organometallics 25 (2006) 1676−1688.

[6] M. Enamullah, G. Makhloufi, R. Ahmed, B.A. Joy, M.A. Islam, D. Padula, H. Hunter, G. Pescitelli, C. Janiak, Synthesis, X-ray, and spectroscopic study of dissymmetric tetrahedral zinc(II) complexes from chiral Schiff base naphthaldiminate ligands with apparent exception to the ECD exciton chirality, Inorg. Chem. 55 (2016) 6449−6464.

[7] N.C. Habermehl, P.M. Angus, N.L. Kilah, L. Norén, A.D. Rae, A.C. Willis, S.B. Wild, Asymmetric transformation of a double-stranded, dicopper(I) helicate containing achiral bis(bidentate) Schiff bases, Inorg. Chem. 45 (2006) 1445−1462.

[8] L.B. Schenkel, J.A. Ellman, Application of *P,N*-sulfinyl imine ligands to iridium-catalyzed asymmetric hydrogenation of olefins, J. Org. Chem. 69 (2004) 1800−1802.

[9] M.J. Chow, C. Licona, D.Y.Q. Wong, G. Pastorin, C. Gaiddon, W.H. Ang, Discovery and investigation of anticancer ruthenium–arene Schiff-base complexes via water-promoted combinatorial three-component assembly, J. Med. Chem. 57 (2014) 6043−6059.

[10] W.-G. Jia, H. Zhang, T. Zhang, D. Xie, S. Ling, E.H. Sheng, Half-sandwich ruthenium complexes with Schiff-base ligands: syntheses, characterization, and catalytic activities for the reduction of nitroarenes, Organometallics 35 (2016) 503−512.

[11] F.E. Fernández, M.C. Puerta, P. Valerga, Ruthenium(II) picolyl-NHC complexes: synthesis, characterization, and catalytic activity in imine *N*-alkylation and transfer hydrogenation reactions, Organometallic 31 (2012) 6868−6879.

[12] L. Ackermann, Metal-catalyzed direct alkylations of (hetero)arenes *via* C–H bond cleavages with unactivated alkyl halides, Chem. Commun. 46 (2010) 4866–4877.

[13] L. Ackermann, Robust ruthenium(II)-catalyzed C–H arylations: carboxylate assistance for the efficient synthesis of angiotensin-II-receptor blockers, Org. Pross. Res. Dev. 19 (2015) 260–269.

[14] P. Pelagatti, M. Carcelli, F. Calbiani, C. Cassi, L. Elviri, C. Pelizzi, U. Rizzotti, D. Rogolino, Transfer hydrogenation of acetophenone catalyzed by half-sandwich ruthenium(II) complexes containing amino amide ligands. Detection of the catalytic intermediates by electrospray ionization mass spectrometry, Organometallics 24 (2005) 5836–5844.

[15] O. Tutusaus, S. Delfosse, A. Demonceau, A.F. Noels, R. Núñez, C. Viñas, F. Teixidor, Olefin cyclopropanation catalysed by half-sandwich ruthenium complexes, Tetrahedron Lett. 43 (2002) 983–987.

[16] M.M. Sheeba, M.M. Tamizh, L.J. Farrugia, A. Endo, R. Karvembu, Chiral (η^6-*p*-cymene) ruthenium(II) complexes containing monodentate acylthiourea ligands for efficient asymmetric transfer hydrogenation of ketones, Organometallics 33 (2014) 540–550.

[17] H. Brunner, R. Oeschey, Stereochemistry at the chiral ruthenium atom in half-sandwich compounds of the type [(η^6-Ar)Ru(LL*)L']X and [(η^6-Ar)Ru(LL*)Hal]. X-ray structure analysis of [(η^6-cymene)Ru(LL*)4-mepy]PF_6 and appeal for the proper use of stereochemical terminology, Inorg. Chem. 34 (1995) 3349–3351.

[18] H. Brunner, R. Oeschey, B. Nuber, Synthesis, properties, stereochemistry and crystal structures of diastereomeric benzene-ruthenium(II) complexes with a chiral saicylideneaminato ligand, Dalton Trans. 8 (1996) 1499–1508.

[19] L.-H. Tang, X. Chen, A.-Q. Jia, Z.-F. Xin, Q.-F. Zhang, Synthesis, characterization and crystal structures of ruthenium complexes with bidentate chiral salicylaldiminato ligands, Inorg. Chem. Acta 479 (2018) 120–127.

[20] M.A. Bennett, T.N. Huang, T.W. Matheson, A.K. Smith, Di-μ-chlo-bis[chloro(6-1-isopropyl-4-methyl-bezene)ruthenium(II)], Inorg. Synth. 21 (1982) 75–75.

[21] *SMART and SAINT+ for Windows NT Version 6.02a*. Bruker Analytical X-ray Instruments Inc., Madison, Wisconsin, USA, 1998.

[22] G.M. Sheldrick, Sadabs, University of Göttingen, Göttingen, Germany, 1996.

[23] G.M. Sheldrick. Shelxtl Software Reference Manual (version 5.1), Bruker AXS Inc., Madison, Wisconsin, USA, 1997.

[24] G.M. Sheldrick, A short history of SHELXTL, Acta Crystallogr. A. 64 (2008) 112–122.

[25] R.K. Rath, M. Nethaji, A.R. Chakravarty, Synthesis, crystal structure and solution properties of a diastereomeric (*p*-cymene)ruthenium(II) chiral Schiff base complex, Polyhedron 21 (2002) 1929–1934.

[26] R.I. Kureshy, N.H. Khan, Synthesis, spectroscopic and electrochemical studies of mixed ligand ruthenium(II) chiral Schiff base complexes with nitrogen donors, Transit. Metal Chem. 19 (1994) 457–460.

[27] H. Brunner, F. Henning, M. Weber, M. Zabel, D. Carmona, F.J. Lahoz, Enantioselective catalysis; 150: chiral-at-metal (η^6-cymene)ruthenium(II) complexes of binaphthyl ligands–synthesis, characterization, and enantioselective catalysis, Synthesis 7 (2003) 1091–1099.

[28] H. Brunner, T. Zwack, M. Zabel, Optically active transition metal complexes. 130. Synthesis, crystal structures, and catalytic properties of chiral-at-metal (η^6-arene)ruthenium(II) and (η^6-arene)osmium(II) half-sandwich complexes. Crystallization of pure diastereomers versus diastereomer mixtures in a 1:1 ratio, Organometallics 22 (2003) 1741–1750.

[29] J. Ji, X. Chen, H. Lin, A.-Q. Jia, Q.-F. Zhang, Ruthenium(II) complexes with substituted 2-(methylthio)-phenylsalicylaldimine Schiff-base ligands, Inorg. Chem. Acta 494 (2019) 105–111.

[30] W.-J. Ruan, G.-H. Hu, S.-J. Wang, J.-H. Tian, Q.-L. Wang, Z.-A. Zhu, Two novel μ-oxo diiron(III) Schiff base complexes: X-ray diffraction analyses, IR, UV-Vis, CD spectra, magnetic susceptibility and electrochemistry, Chin. J. Chem. 23 (2005) 709–714.

[31] R.C. Felicio, G.A. da Silva, L.F. Ceridorio, E.R. Dockal, Tetradentate Schiff base copper(II) complexes, Synth. React. Inorg. Met. Org. Chem. 29 (1999) 171–192.

[32] K. Stanley, M.C. Baird, A demonstration of controlled asymmetric induction in organoiron chemistry. Suggestions concerning the specification of chirality in pseudotetrahedral metal complexes containing polyhapto ligands, J. Am. Chem. Soc. 97 (1975) 6598–6599.

[33] Y.-J. Yang, X.-X. Ge, L.-H. Guo, T. Zhu, Z.-Z. Tian, H.-R. Zhang, Q. Du, H.-W. Peng, W.-L. Ma, Z. Liu, Zwitterionic and cationic half-sandwich iridium(III) ruthenium(II) complexes bearing sulfonate groups: synthesis, characterization and their different biological activity, Dalton Trans. 48 (2019) 3193–3197.

[34] M. Muralisankar, R. Dheepika, J. Haribabu, C. Balachandran, S. Aoki, N.S.P. Bhuvanesh, S. Nagarajan, Design, Synthesis, DNA/HSA binding, and cytotoxic activity of half-sandwich Ru(II)-arene complexes containing triarylamine−thiosemicarbazone hybrids, ACS Omega 4 (2019) 11712–11723.

[35] A. Gatti, A. Habtemariam, I. Romero-Canelón, J.I. Song, B. Heer, G.J. Clarkson, D. Rogolino, P.J. Sadler, M. Carcelli, Half-sandwich arene ruthenium(II) and osmium(II) thiosemicarbazone complexes: solution behavior and antiproliferative activity, Organometallics 37 (2018) 891–899.

[36] J. Hildebrandt, H. Görls, N. Häfner, G. Ferraro, M. Dürst, I.B. Runnebaum, W. Weigand, A. Merlino, Unusual mode of protein binding by a cytotoxic π-arene ruthenium(II) piano-stool compound containing an *O,S*-chelating ligand, Dalton Trans. 45 (2016) 12283–12287.

[37] H. Mishra, A.K. Patra, R. Mukherjee, Relative stability of half-sandwich η^6-benzene Ru(II) complexes of tridentate (2-pyridyl)alkylamine ligands of varying chelate ring-size: nucleophilic addition of hydride ion onto the benzene ring, Inorg. Chim. Acta 362 (2009) 483–490.

[38] M. Ramesh, G. Venkatachalam, Half–sandwich (η^6–*p*–cymene) ruthenium(II) complexes bearing 5–amino–1–methyl–3–phenylpyrazole Schiff base ligands: synthesis, structure and catalytic transfer hydrogenation of ketones, J. Organomet. Chem. 880 (2019) 47–55.

[39] H. Brunner, R. Oeschey, B. Nuber, Optically active transition metal complexes. Part 108. Synthesis, crystal structure and properties of a novel 'quasi-meso' dinuclear η^6-benzene-ruthenium(II) complex with chiral salicylaldiminato ligands, J. Organomet. Chem. 518 (1996) 47–53.

Table 1. Crystallographic data and experimental details for **HL1***–**HL7*** and (*S*)-[(η^6-*p*-cymene)Ru(κ^2-*N*,*O*-**L3***)Cl] (**3**)

Complex	**HL1***	**HL2***	**HL3***	**HL4***	**2(HL5*)·0.5H$_2$O**	**HL6***	**HL7***	**3**
Empirical formula	$C_{12}H_{17}NO_2$	$C_{12}H_{16}N_2O_4$	$C_{23}H_{31}NO$	$C_{15}H_{13}NOBr$	$C_{20}H_{23}N_2O_{4.5}Br_4$	$C_{12}H_{15}NO_2Br_2$	$C_{10}H_{11}NO_2Br_2$	$C_{33}H_{43}NOClRu$
Formula weight	207.27	252.27	337.49	383.09	683.04	365.11	413.11	606.20
Crystal system	Rhombohedral	Orthorhombic	Orthorhombic	Monoclinic	Triclinic	Monoclinic	Monoclinic	Triclinic
a (Å)	23.479(9)	7.542(3)	6.293(3)	22.04(3)	6.7964(15)	7.3140(10)	14.856(4)	9.6395(16)
b (Å)	23.479(9)	10.796(4)	9.885(5)	9.333(11)	8.8071(19)	22.257(3)	7.020(2)	10.1718(17)
c (Å)	6.014(5)	32.777(11)	34.912(18)	15.541(19)	11.479(2)	8.7700(12)	16.709(5)	17.607(3)
α (°)					109.685(2)			83.990(2)
β (°)				112.331(15)	98.581(3)	93.030(2)	112.071(3)	80.670(2)
γ (°)	120				101.767(2)			63.684(2)
V (Å^3)	2871(3)	2668.8(15)	2171.6(19)	2957(6)	615.4(2)	1425.7(3)	1614.9(8)	1525.9(4)
Space group	*R*3	$P2_12_12_1$	$P2_12_12_1$	*C*2	*P*1	$P2_1$	$P2_1$	*P*$\bar{1}$
Z	9	8	4	8	1	4	4	2
D_{calc} (g cm^{-3})	1.079	1.256	1.032	1.721	1.843	1.691	1.699	1.319
Temperature (K)	296(2)	296(2)	296(2)	296(2)	296(2)	296(2)	296(2)	296(2)
F(000)	1008	1072	736	1504	333	712	816	634
μ(Mo-Kα) (mm^{-1})	0.073	0.095	0.062	5.474	6.570	5.676	5.023	0.626
Total refln	6088	16788	13462	8923	3797	8868	9938	9586
Independent refln	3002	6054	4837	6177	3173	4648	5384	6713
R_{int}	0.0329	0.1256	0.0340	0.0583	0.0164	0.0263	0.0405	0.0383

$R1$[a], $wR2$[b] ($I > 2\sigma(I)$)	0.0481, 0.1106	0.0757, 0.1426	0.0662, 0.1821	0.0520, 0.1119	0.0369, 0.0797	0.0375, 0.0781	0.0381, 0.0809	0.0687, 0.1732
$R1$, $wR2$ (all data)	0.1208, 0.1433	0.2904, 0.2184	0.1298, 0.2240	0.1404, 0.1431	0.0550, 0.0851	0.0766, 0.0890	0.0582, 0.0891	0.0978, 0.1995
GoF[c]	0.893	0.894	1.023	0.904	0.984	1.004	1.009	1.055
Flack parameter	0.5(10)	2.0(10)	-1.5(10)	0.022(17)	0.028(16)	0.007(10)	0.001(9)	-

[a] $R1 = \Sigma \left| |F_o| - |F_c| \right| / \Sigma |F_o|$.
[b] $wR2 = [\Sigma w(|F_o^2| - |F_c^2|)^2 / \Sigma w |F_o^2|^2]^{1/2}$.
[c] $\mathrm{GoF} = [\Sigma w(|F_o| - |F_c|)^2 / (N_{obs} - N_{param})]^{1/2}$.

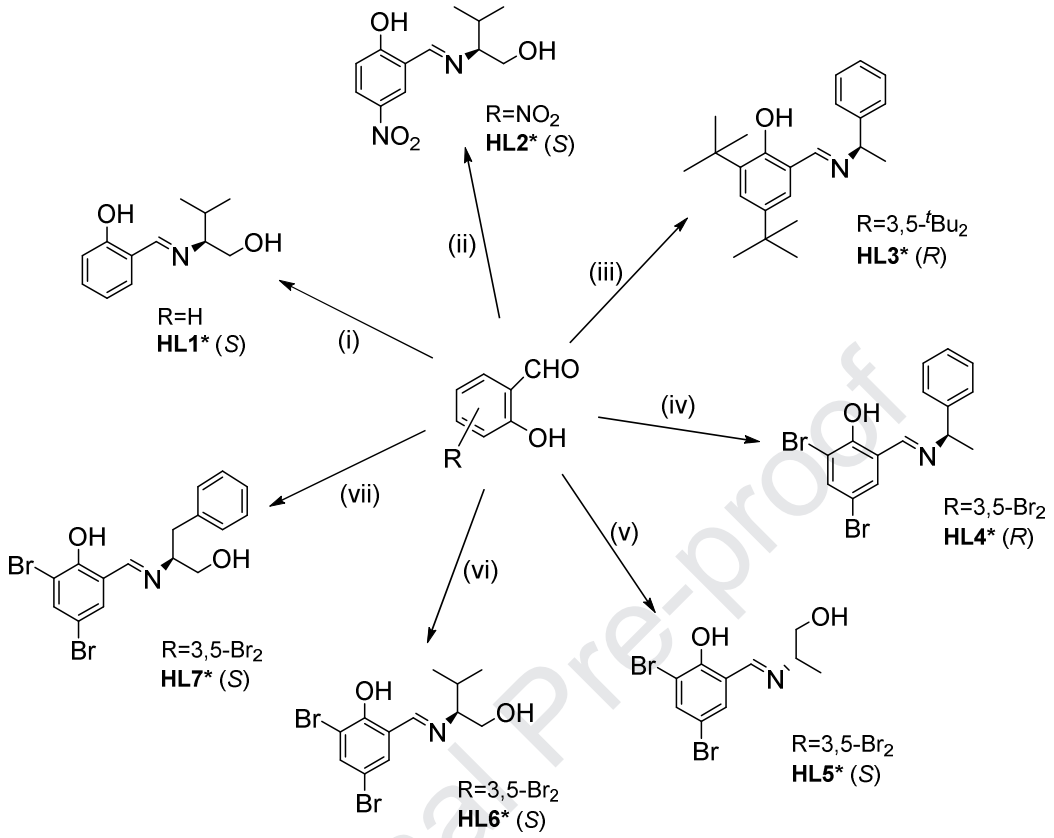

Scheme 1. Syntheses of chiral Schiff bases **HL1***–**HL7***. Reagents and conditions: (i) (*S*)-(+)-2-amino-3-methyl-1-butanol, ethanol, at reflux; (ii) (*S*)-(+)-2-amino-3-methyl-1-butanol, ethanol, at reflux; (iii) (*R*)-(+)-α-methylbenzylamine, ethanol, at reflux; (iv) (*R*)-(+)-α-methylbenzylamine, ethanol, at reflux; (v) (*S*)-(+)-2-amino-1-propanol, ethanol, at reflux; (vi) (*S*)-(+)-2-amino-3-methyl-1-butanol, ethanol, at reflux; (vii) (*S*)-(-)-2-amino-3-phenyl-1-propanol, ethanol, at reflux.

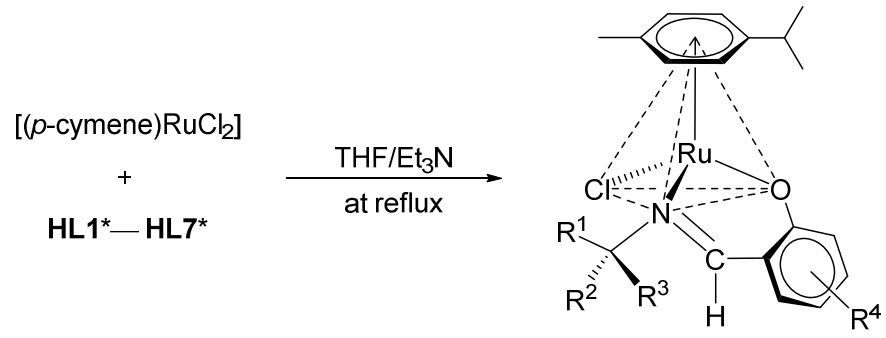

R^1=isopropyl, R^2=hydroxymethyl, R^3=H, R^4=H	**1**
R^1=isopropyl, R^2=hydroxymethyl, R^3=H, R^4=NO_2	**2**
R^1=Ph, R^2=Me, R^3=H, R^4=3,5-^{t}Bu$_2$	**3**
R^1=Ph, R^2=Me, R^3=H, R^4=3,5-Br_2	**4**
R^1=Me, R^2=hydroxymethyl, R^3=H, R^4=3,5-Br_2	**5**
R^1=isopropyl, R^2=hydroxymethyl, R^3=H, R^4=3,5-Br_2	**6**
R^1=CH_2Ph, R^2=hydroxymethyl, R^3=H, R^4=3,5-Br_2	**7**

Scheme 2. Syntheses of half-sandwich ruthenium(II) complexes **1**–**7**.

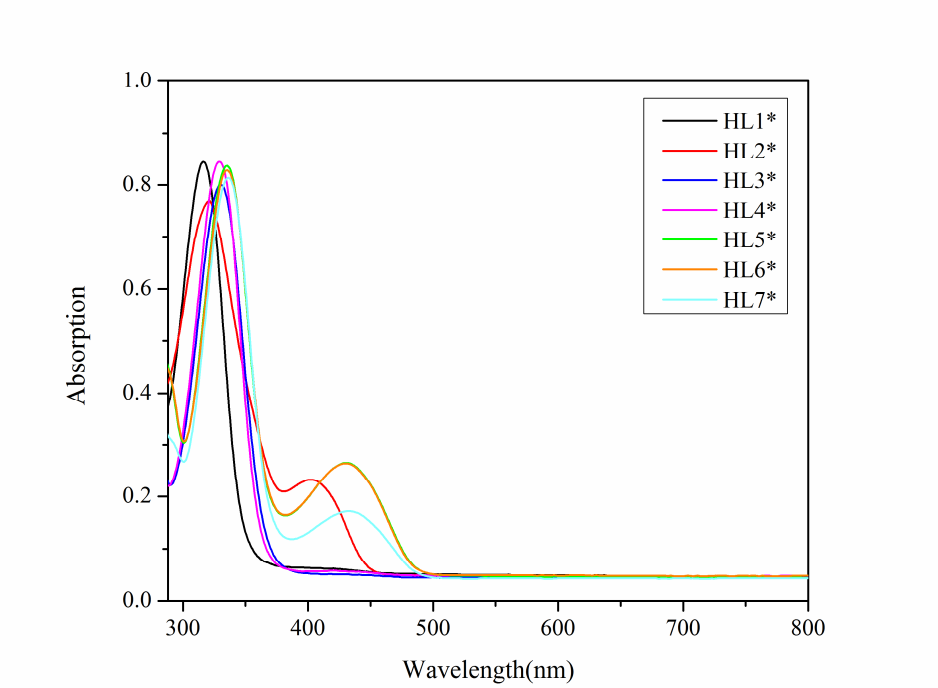

Fig. 1. UV/Vis spectra of chiral Schiff bases **HL1***–**HL7*** measured in dichloromethane.

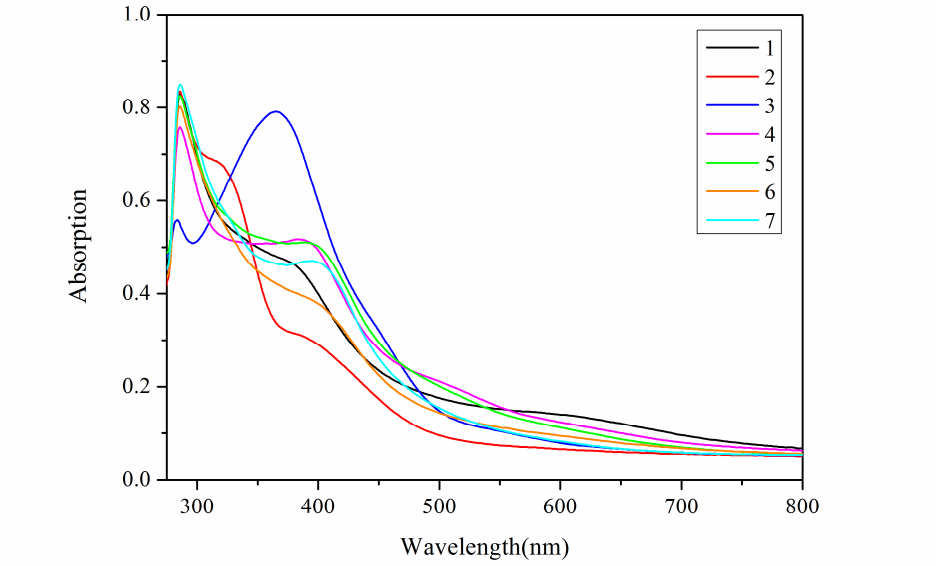

Fig. 2. UV/Vis spectra of half-sandwich ruthenium(II) complexes **1**–**7** measured in dichloromethane.

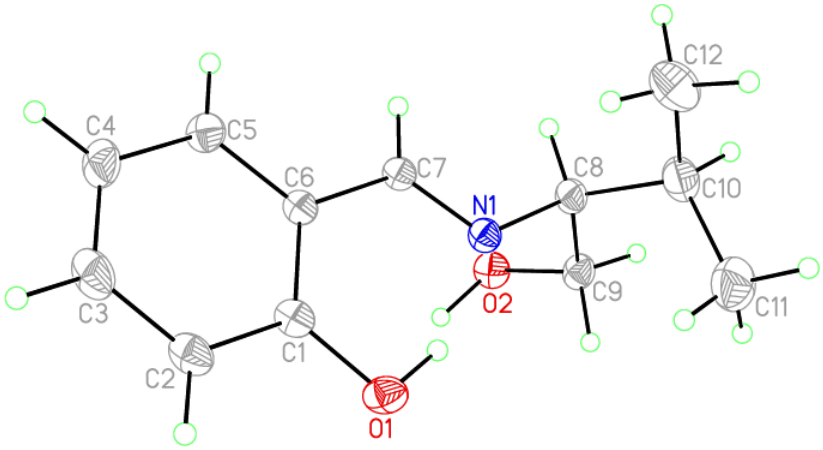

Fig. 3. ORTEP diagram of (*R*)-*N*-(1-hydroxymethylisobuty)salicylidene (**HL1***), showing the atom labeling scheme and 40% thermal ellipsoids. Selected bond lengths (Å) and angles (deg): O(1)-C(1) 1.354(4), N(1)-C(7) 1.276(3), N(1)-C(8) 1.461(3).

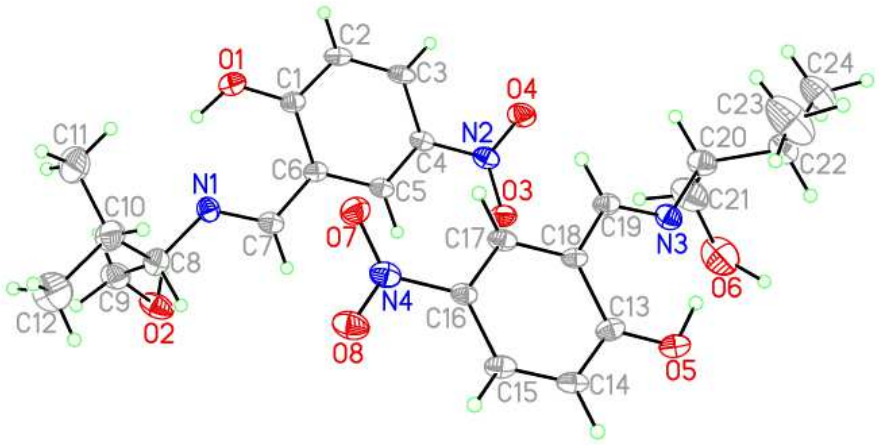

Fig. 4. ORTEP diagram of (*R*)-*N*-(1-hydroxymethylisobuty)(5-nitrosalicylidene) (**HL2***). Selected bond lengths (Å) and angles (deg): O(1)-C(1) 1.271(7), N(1)-C(7) 1.275(7), N(1)-C(8) 1.450(8), O(5)-C(13) 1.286(7), N(3)-C(19) 1.293(7), N(3)-C(20) 1.469(8).

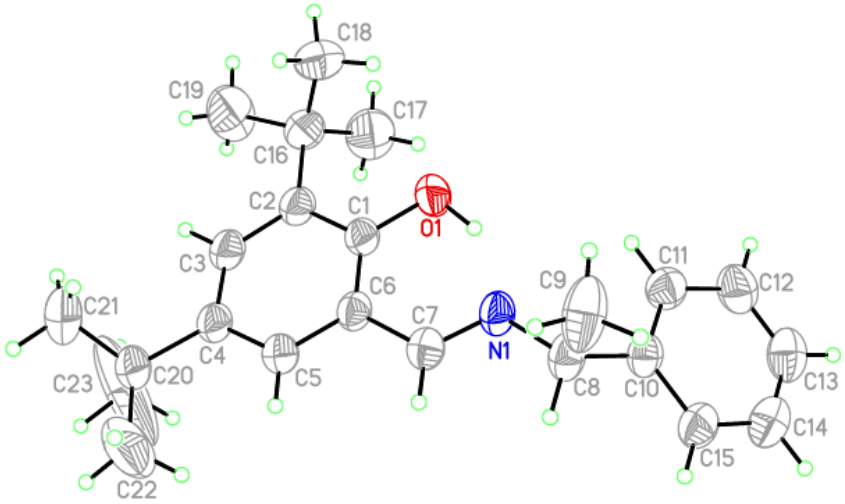

Fig. 5. ORTEP diagram of (*R*)-*N*-(1-phenylethyl)(3,5-di-*tert*-butylsalicylidene) (**HL3***), showing the atom labeling scheme and 40% thermal ellipsoids. Selected bond lengths (Å) and angles (deg): O(1)-C(1) 1.352(3), N(1)-C(7) 1.265(4), N(1)-C(8) 1.455(4).

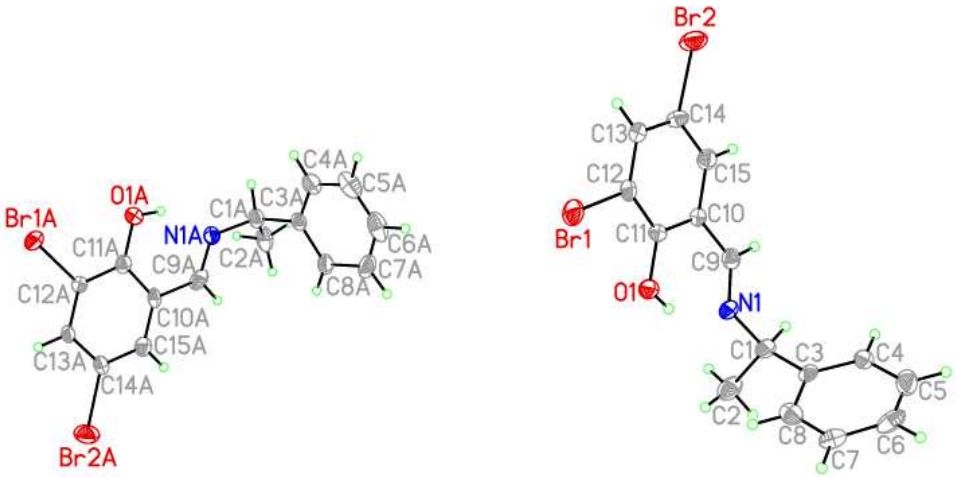

Fig. 6. ORTEP diagram of (*R*)-*N*-(1-phenylethyl)(3,5-dibromosalicylidene) (**HL4***), showing the atom labeling scheme and 40% thermal ellipsoids. Selected bond lengths (Å) and angles (deg): O(1)-C(11) 1.355(10), N(1)-C(1) 1.487(9), N(1)-C(9) 1.242(11), O(1A)-C(11A) 1.330(11), N(1A)-C(1A) 1.477(9), N(1A)-C(9A) 1.269(11).

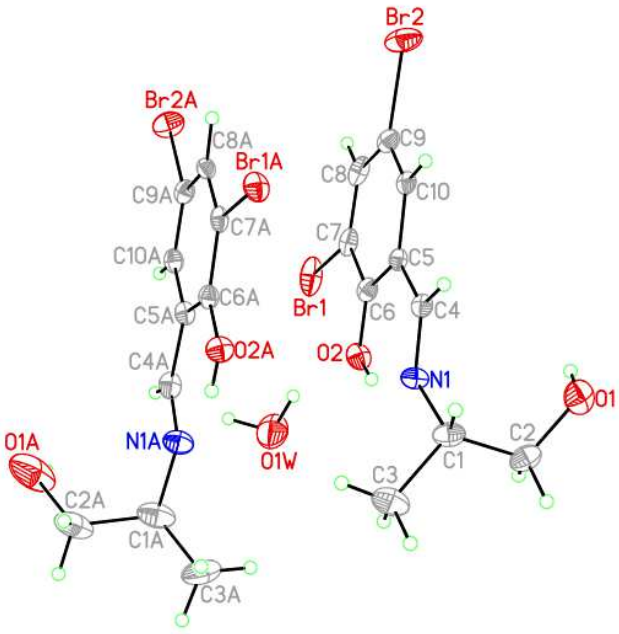

Fig. 7. ORTEP diagram of (*S*)-*N*-(1-hydroxymethylethyl)(3,5-dibromosalicylidene) (**HL5***), showing the atom labeling scheme and 40% thermal ellipsoids. Selected bond lengths (Å) and angles (deg): O(1)-C(2) 1.420(10), N(1)-C(1) 1.494(10), N(1)-C(4) 1.300(8), O(2A)-C(6A) 1.289(8), N(1A)-C(1A) 1.471(10), N(1A)-C(4A) 1.331(10).

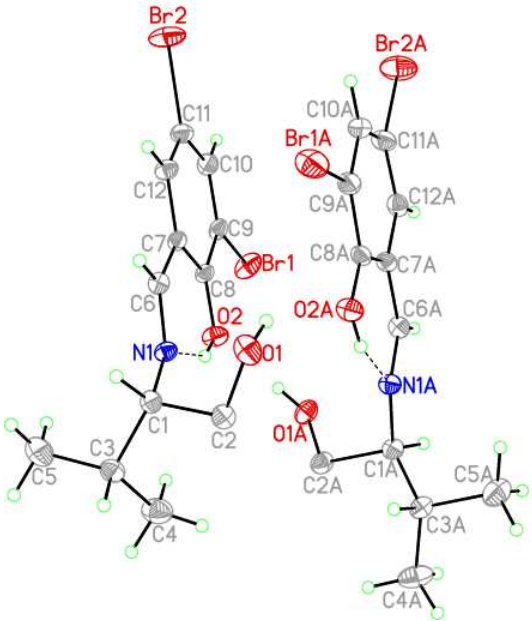

Fig. 8. ORTEP diagram of (*R*)-*N*-(1-hydroxymethylisobutyl)(3,5-dibromosalicylidene) (**HL6***), showing the atom labeling scheme and 40% thermal ellipsoids, O–H···N intermolecular hydrogen bonds are depicted as dashed lines. Selected bond lengths (Å) and angles (deg): O(2)-C(8) 1.280(6),

N(1)-C(1) 1.473(6), N(1)-C(6) 1.288(6), O(2A)-C(8A) 1.275(6), N(1A)-C(1A) 1.452(7), N(1A)-C(6A) 1.278(7).

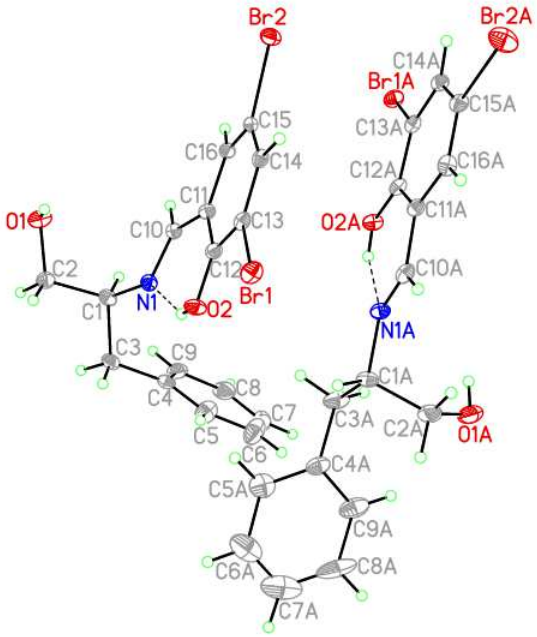

Fig. 9. ORTEP diagram of (*S*)-*N*-(1-hydroxymethylphenyl)(3,5-dibromosalicylidene) (**HL7***), showing the atom labeling scheme and 40% thermal ellipsoids, O–H···N intermolecular hydrogen bonds are depicted as dashed lines. Selected bond lengths (Å) and angles (deg): O(2)-C(12) 1.274(6), N(1)-C(1) 1.463(7), N(1)-C(10) 1.305(6), O(2A)-C(12A) 1.280(6), N(1A)-C(1A) 1.489(7), N(1A)-C(10A) 1.267(7).

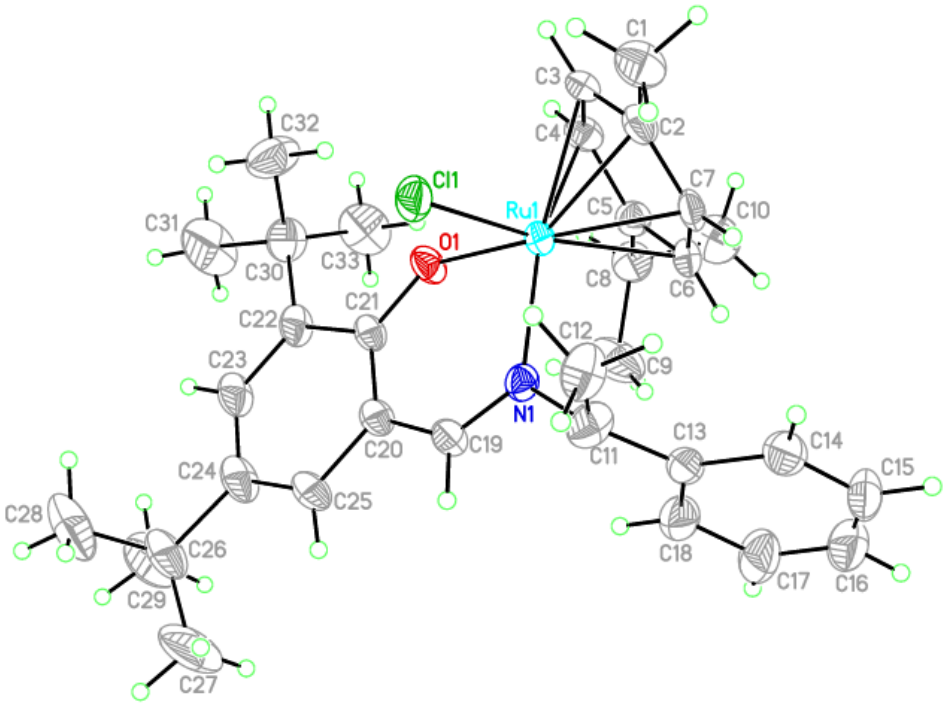

Fig. 10. Molecular structure of half-sandwich ruthenium(II) complex **3**. Thermal ellipsolids are shown at the 40% probability level. Selected bond lengths (Å) and angles (deg): Ru(1)-C_{av} 2.198(6), Ru(1)-O(1) 2.054(4), Ru(1)-N(1) 2.117(5), Ru(1)-Cl(1) 2.4190(16), O(1)-C(21) 1.289(6), N(1)-C(19) 1.303(7), N(1)-C(11) 1.482(7), C(19)-C(20) 1.418(8), C(20)-C(21) 1.418(8), O(1)-Ru(1)-N(1) 88.21(17), O(1)-Ru(1)-Cl(1) 85.75(13), N(1)-Ru(1)-Cl(1) 82.10(14), C(11)-N(1)-Ru(1) 119.8(4), C(19)-N(1)-C(11) 117.4(5), C(19)-N(1)-Ru(1) 122.6(4), C(11)-N(1)-Ru(1) 119.8(4), C(21)-O(1)-Ru(1) 130.8(4), O(1)-C(21)-C(20) 123.2(5), C(21)-C(20)-C(19) 124.0(5), N(1)-C(19)-C(20) 130.4(6).

Graphical Abstract

Synthesis, characterization and crystal structures of half-sandwich ruthenium complexes with bidentate chiral Schiff-base ligands

Chong Chen, Jiao Ji, Chang-Jiu Wang, Ai-Quan Jia, and Qian-Feng Zhang*

A series of chiral Schiff base ligands and the corresponding half-sandwich ruthenium(II) complexes were synthesized and characterized by single-crystal X-ray diffraction and their electronic absorption spectra were also investigated.

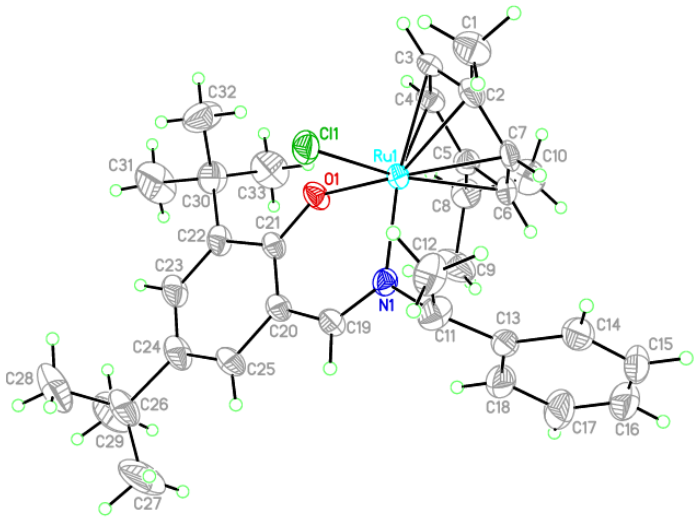

Highlights

► Seven chiral N^O ligands were characterized by single-crystal X-ray crystallography.

► The corresponding half-sandwich ruthenium(II) complexes were synthesized.

► The electronic absorption spectra of these ruthenium complexes were investigated.

Declaration of interests

☒ The authors declare that they have no known competing financial interests or personal relationships that could have appeared to influence the work reported in this paper.